Fuel 141 (2015) 275–284

Prediction of biomass ash fusion behaviour by the use of detailed characterization methods coupled with thermodynamic analysis.

T. Rizvi, P. Xing, M. Pourkashanian, L.I. Darvell, J.M. Jones, W. Nimmo

*Corresponding author. E-mail address: w.nimmo@sheffield.ac.uk

Abstract

Ash deposition such as slagging and fouling on boiler tube surfaces is an inevitable, though undesirable consequence of burning solid fuels in boilers. The role of fuel characteristics, in affecting the form and severity of the problem, is significant. In recent years, biomass fuels have gained increasing popularity as an environmentally friendly source of energy in power plants all over the world. This study is based on characterising the fusion behaviour of four biomass fuels (pine wood, peanut shells, sunflower stalk and miscanthus) using ash fusion temperature (AFT) tests, simultaneous thermal analysis (STA) of fuel ashes, calculation of empirical indices and predicting ash melting behaviour with the help of thermodynamic equilibrium calculations. The AFT results failed to show any clear trend between fusion temperature and high alkali content of biomass. STA proved useful in predicting the different changes occurring in the ash. Empirical indices predicted high slagging and fouling hazards for nearly all the biomass samples and this was supported by the possible existence of a melt phase at low temperatures as predicted by thermodynamic calculations.

Keywords: Ash deposition, fusion behaviour, simultaneous thermal analysis, thermodynamic equilibrium.

Introduction

During the past decade, the use of biomass fuels for energy generation has gained increasing significance as a ‘carbon neutral’ source of energy following the global greenhouse gas(GHG) emission reduction constraints implemented on power plants worldwide. Biomass co-firing in coal based thermal power plants is known to reduce the emission of harmful pollutants such as the oxides of carbon, sulphur and nitrogen as well as the release of toxic substances such as mercury[1-4]. However, there are a few disadvantages associated with biomass firing and co-firing which include slightly higher plant operating costs, a modest decrease in boiler efficiency (derating) and a potential increase in ash related problems such as slagging, fouling and high temperature corrosion of heat transfer surfaces [5-7].

The propensity of fuels to slag and foul boiler heat transfer surfaces can be predicted by means of laboratory based tests and measurements. Commonly used analytical techniques include testing the fusion characteristics of ash, measurements of ash viscosity and estimation of indices based on ratios of elemental oxides[8-10]. Despite the limitations associated with

these techniques, they are still widely used to assess the tendency of various coals to slag and foul boiler heat transfer surfaces and have also been extended to biomass fuels for evaluation of the same[11-14].

The details regarding the various mechanisms associated with deposit formation and important elements and mineral species in fuels that contribute to slagging and fouling are well documented in the literature [15-19]. A number of these studies reveal that the formation of an initial melt phase greatly expedites the accumulation of ash deposits on boiler tubes, with a melt phase of as little as 10% enough to initiate extensive deposit formation [20]. Ash fusion temperature(AFT) testing is a widely used laboratory technique in this regard, since it gives an indication of the melting behaviour of ash with respect to temperature. While ash fusion measurements take into account visual changes such as change in shape of specimen caused by viscosity changes, improved knowledge of change in mass of the ash on heating, gas phase release etc can be obtained by techniques such as simultaneous thermal analysis.

The behaviour of ash forming species at high temperatures can also be assessed with the help of thermodynamic equilibrium modelling software, Factsage. Chemical equilibrium calculations can be used to predict the fraction of molten phase in ash and the phase changes associated with the ash fusion temperatures can be correlated with thermodynamic modelling of phase equilibria. Huggins[21] related liquidus temperatures in ternary equilibrium phase diagrams of SiO_2-Al_2O_3-XO (where X= Fe, Ca or K_2) to the AFTs of coal ashes. Jak [22] predicted the coal ash fusion characteristics of a suite of coals by employing the multicomponent system Al-Ca-Fe-O-Si with the help of FACT thermodynamic computer package. Li et al.[23] used Factsage to predict the ash fusion characteristics of certain coals under reducing conditions. While other researchers have employed this technique to predict coal ash fusibility[24], mineral element evaporation[25] and [26-28], research on its applicability to biomass ash and blends is somewhat sparse. Also, the wide variation in composition of different types of biomass, makes it difficult to generalize the results reported in literature. Due to the wide variation in the different types of biomass and their associated characteristics, the need to examine the properties of individual fuels is important in order that data may be used in the assessment of suitability of commercially available biomass for use in power stations.

The present study was conducted in order to assess the behaviour of 4 different biomass fuel ashes with regards to their fusion characteristics and slagging and fouling propensities. This entailed compositional analysis of the fuels, evaluation of empirical indices and ash fusion tests. In addition, the weight loss properties of the ashes and were also studied using Simultaneous Thermal Analysis coupled with Mass Spectrometry(STA-MS). An attempt to evaluate the applicability of phase equilibrium approach to these biomass fuels, with the help of thermodynamic equilibrium software FactSage V6.3, is also presented. Thermodynamic equilibrium calculations are also used to predict the percentage of melt phase at different temperatures in combustion environments and the possible solid phases that are likely to exist at different temperatures.

2.Materials and methods

2.1. Materials

The materials used for this study consisted of 4 biomass samples obtained from a leading UK electricity generator. Out of these biomass samples, soft wood (pine) is a typical example of sustainably produced woody biomass from managed forests and forestry residues. Peanut and sunflower husks represent agricultural residues and by-products of food production that are readily available. Miscanthus is an example of short rotation energy crop that is planted specifically for the purpose of producing energy. The results of the proximate and ultimate analysis of these fuels are shown in Table 1.

2.2 Experimental methods

The samples were ashed using British Standards (BS EN 14775:2009) for solid biofuels. They were first oven dried at 105^0C for 2hrs to remove moisture. The composition of major elements Al_2O_3, SiO_2, K_2O, CaO, Fe_2O_3, Na_2O, MgO, P_2O_5, SO_3, TiO_2 was obtained with the help of X-Ray fluorescence(XRF) analysis. The ash was then analysed as follows:

2.2.1 Ash fusion temperature(AFT) testing

Ash fusion tests were carried out in a Carbolite Ash Fusion furnace fitted with a camera and image processing software designed to capture images at preset temperature intervals. The samples were prepared by carefully adding a few drops of demineralised water to the ash to form a paste of suitable consistency. They were then moulded into compact cylinders 5mm(height) and 5mm(dia) and allowed to dry. The ash test pieces were then mounted on porcelain slabs and placed inside the furnace and heated in an oxidising environment (air) at a constant heating rate of 10^0C/min from 550^0C to 1500^0C. The digital probe fitted inside the furnace enabled image capture at every 5^0C rise in temperature. The key stages in the deformation and flow of the sample cylinders were determined using European Standards (DD CEN/TS 15370 – 1:2006) [29]. The shrinkage temperature(ST) is defined as the temperature at which the area of the test piece reduces to 95% of the original area. The temperature at which the first signs of rounding of the edges occur, marks the deformation temperature(DT). The hemispherical temperature(HT) is the temperature at which the height becomes approximately half of the base diameter such that the test piece forms a hemisphere. At the flow temperature(FT), the height of the melting ash layer becomes approximately half the height at the hemisphere temperature.

2.2.2 Simultaneous Thermal Analysis coupled with Mass Spectrometry (STA-MS)

Simultaneous thermal analysis enables the application of thermogravimetry (TG) alongside differential thermal analysis (DTA) in a single equipment. This approach for analysis has been used before by Baxter et al. [30]. The ash samples were analyzed using a Netzsch STA (Simultaneous Thermal Analysis) 449C coupled with a Netzsch QMS(Quadrupole Mass Spectrometer) 403C Aeolos equipment. Thermogravimetric analysis gives information on the mass change occurring in a sample under a controlled heating programme while differential thermal analysis provides insight into the heat producing(exothermic) and heat consuming(endothermic) reactions taking place in the sample by comparison with an inert

reference material. In each case, 10mg of ash was heated from 30^0 to 1400^0C in a 12.5% O_2/He environment at a constant heating rate of 10^0C/min. The gas outlet at the furnace of the thermobalance was connected to the gas inlet at the mass spectrometer through a heated fused silica capillary tube. This enabled the detection of gas species such as carbon dioxide, sulphur dioxide, chlorine and water vapour, evolved during the heating process.

2.2.3 Thermodynamic Modelling

Thermodynamic prediction of the equilibrium phases formed during the ash fusion process was performed using FactSage 6.3 thermochemical software and databases [31-33]. Factsage is one of the most commonly used programme packages for calculating multicomponent, multiphase equilibria for various systems. It contains extensive thermochemical databases for use with different modules. For this study, the 'Equilib' module was employed along with FToxid and FactPS databases. The C,H,N, O, and ash content of the fuels in terms of major oxides Al_2O_3, SiO_2, K_2O, CaO, Fe_2O_3, Na_2O, MgO, P_2O_5, SO_3 were used as inputs in the Reactants window of the programme. The calculations were carried out under oxidizing conditions such that V/V_0 (ratio of actual to theoretical air input) was set at 1.15 for all the cases. The temperature range of 700^0C to 1500^0C was selected yielding 9 subsets of data for each fuel at a temperature interval of 100^0C.

3. Results and discussion

3.1 Elemental Analysis of ash and calculated ash fusibility indices

The composition of ash in terms of oxides of major elements is shown in Table 2, along with calculated indices. It can be observed that there is a wide variation in the elemental composition of the different ashes. Out of the four biomasses, wood and miscanthus are high in silica content at 45.52 and 49.55% respectively followed by peanut husk at 35.55%. The alumina content of all the biomasses is low, while the potassium content is considerably high as would be expected for biomass fuels. All of the biomasses also possess considerable calcium content. Sunflower stalk is the only low alumina, low silica biomass containing appreciable amounts of potassium, calcium and magnesium.

The following indices are calculated:

Base to acid ratio

$$R_{B/A} = \frac{Fe_2O_3 + CaO + MgO + Na_2O + K_2O}{SiO_2 + Al_2O_3 + TiO_2} \quad (1)$$

Slag viscosity index

$$S_R = \frac{SiO_2}{SiO_2 + Fe_2O_3 + CaO + MgO} \times 100 \quad (2)$$

Fouling index

$$F_U = R_{B/A} \times (Na_2O + K_2O) \quad (3)$$

Alkali Index

$$AI = \frac{kg(Na_2O + K_2O)}{GJ} \quad (4)$$

The corresponding slagging or fouling tendencies have been marked as severe(S), medium(M), high(H) and low(L) where possible according to data available in literature [34-36]. Although the values of $R_{B/A,}$ S_R and F_U for sunflower ash are rather peculiar owing to its very different composition, they tend to lean towards the high slagging tendencies. On the whole, all of the calculated indices predict consistently high slagging and fouling tendencies for almost all of the biomasses except for two marginal exceptions. Wood has a low alkali index owing to the lower alkali content (K and Na) while miscanthus exhibits a low slag viscosity index owing to its comparatively low alkaline earth metal content (Ca and Mg). It is interesting to note that although the predicted slagging and fouling potential depicted by these indices are mostly based on values obtained from coals, they seem to show good agreeability with one another for the biomass samples considered in this study.

3.2 Ash fusion tests

Table 3 shows the three key temperatures during the different stages in melting of the four fuels ashes. The shrinkage temperature has not been reported due to the difficulty in discerning accurately such a small change in area due to poor luminosity at lower temperatures resulting in images with very low contrast ratio. The results of AFT for the present biomass samples do not show a clear relation between high K content and low melting temperatures observed by Werther et al. [37] using samples of oat, rye and barley. On the contrary, it is interesting to note that although miscanthus and peanut have similar K content, there is a marked variation in their fusion temperatures. Also, sunflower ash despite possessing the highest K content, does not display low melting temperatures. Conversely, it exhibits the highest fusion temperatures. This suggests that the melting temperatures obtained from AFT studies cannot be expressed as a simple function of potassium content for all types of biomass.

3.3 Simultaneous Thermal Analysis

The results obtained from STA-MS tests from wood, peanut, sunflower and miscanthus ash are presented in Figure 1, Figure 2, Figure 3 and Figure 4 respectively. The mass loss and DTA curves are representative of physical and chemical changes taking place in the samples with melting and evaporation being dominant[38]. It is evident that all of the samples show distinct regions of mass loss except miscanthus which shows varying mass loss over the entire temperature range. In the low temperature window (below 500^0C), wood and sunflower ash samples do not exhibit any significant mass loss. The mass loss associated with peanut and miscanthus ash in this temperature range can be attributed to the evaporation of absorbed

moisture from hygroscopic compounds such as K_2CO_3 that are likely to be present in some biomass ashes [30].

In the temperature region 500-1000^{0}C, mass loss is most likely due to the thermal decomposition of $CaCO_3$ particularly between 600-800^{0}C [39].

$$CaCO_3 \rightarrow CaO + CO_2 \uparrow$$

This is evidenced by the corresponding CO_2 peaks in both wood and sunflower. However, this cannot be generalized for all the ashes since only a very slight CO_2 peak is observed for the peanut ash and none for miscanthus. For these ashes mass loss could be due to the evaporation of other species either by reactions within the ash or volatilization of active compounds. For instance, KCl is known to evaporate above 700^{0}C and was found to be one of the main crystalline species present in high K containing biomass ashes by Du et al [40].

In the high temperature range (above 1000^{0}C) CO_2 and H_2O are progressively released into the gas phase for all the ashes. The remarkable similarity in the trend of the signal intensities for all cases suggests the occurrence of similar reactions. One probability could be the dehydroxylation and decarbonotation of lattice compounds in complex mineral species and the destruction of their structure, that can occur at high temperatures[41]. An increase in the SO_2 signal, as well as that of Cl can also be observed in all cases, mainly above 1200^{0}C. This can be attributed to their release from the breakdown of complex high temperature mineral and inorganic species in the ash.

The minimum endothermic temperatures for the ashes as estimated from the DTA curves are shown in Table 4. The upward slope of the STA curve represents exothermic reactions while the downward sloping section is attributed to endothermic processes. The shift from exothermic to endothermic conditions on the curve is indicative of melting. The minimum endothermic temperatures evaluated in this way are much lower than the corresponding initial deformation temperatures obtained from ash fusion tests. This is in agreement with the findings of Wall et al.[8] who used alternative laboratory techniques to conclude that the initial deformation temperature cannot be regarded as the lowest temperature for ash to soften. On the other hand, the minimum endothermic temperature cannot automatically be assumed to represent the temperature where melting first starts. Since it represents the initiation of net endothermic conditions, the probability of simultaneous exothermic and endothermic reactions below this temperature and vice versa cannot be disregarded.

3.4 Thermodynamic equilibrium predictions

Figure 5 shows the relative amounts of liquid slag formation for the different fuels under oxidising conditions as predicted with the help of Factsage 6.3. These results show the presence of a liquid phase even at 700^{0}C for all the biomasses. Interestingly, however, the amount of liquid slag does not increase with temperature for all the cases. For miscanthus it increases upto to 1000^{0}C, remains constant from 1000-1100^{0}C and then decreases. For peanut shells, it remains constant till about 900^{0}C, decreases till 1400^{0}C and then increases again. For wood it remains fairly constant until 1200^{0}C, increasing sharply at 1300 and becoming

stable again with a slight increase at 1400^0C. The most unusual results are encountered in the case of sunflower husks which shows a peak at 900^0C but negligible liquid slag at 1100^0C.

Figure 6 represents the major solid phases in equilibrium with the slag phase at different temperatures. It can be observed that while solid potassium compounds exist below 1100^0C for most of the biomasses, Ca and Mg bearing phosphates and silicates are the main solid species at high temperatures (above 1300^0C). The role of phosphorous in ash melting behaviour is considered important by many researchers but [42] found that phosphorous only helps to lower the melting temperature if the A/CNK ratio (Al_2O_3/CaO+Na_2O+K_2O) is more than 1. Since the A/CNK ratio is less than one for all the biomass samples used in the present study, the presence of solid phosphorous bearing species at high temperatures, as evaluated by Factsage, seems justified.

Figure 7 represents the proportion of major oxides in the slag phase with respect to temperature. The results suggest that K_2O and Si_2O containing species form the major portion of the slag for all the biomasses. It is further noticeable that a decrease of K containing species in the solid phase corresponds to an increase in the K content in the slag phase for wood, peanut and sunflower. However this behaviour cannot be observed for the results obtained for sunflower husk, where no K containing species seem to exist above 1100^0C in either the solid or the liquid phase. This suggests their release into the vapour phase.

4. Conclusions

The ash fusion behaviour of four biomasses having varying compositions was studied with the help of ash fusion tests, simultaneous thermal analysis and thermodynamic equilibrium modelling. A number of empirical indices were also evaluated which showed high slagging and fouling propensities for nearly all the biomass samples. Simultaneous thermal analysis was used to assess the physical & chemical changes taking place in the ash as well as predicting to some extent, the possible reactions involved. Although this data can be interpreted more clearly by coupling it with XRD analysis to identify the different phases present in the ash, simultaneous thermal analysis still provides a more comprehensive explanation of the fusion behaviour of ashes which simpler techniques such as ash fusion tests fail to do. However, the difficulty in linking laboratory data to the prediction of fusion temperatures and slagging and fouling propensities in real boilers still remains. In this regard, thermodynamic equilibrium predictions can be more useful as they take into account the chemical composition of the fuel (and products of combustion) as well as ash. Nevertheless, it is important to consider the limitations associated with each of these techniques before projecting this data for real time assessment of large scale combustion systems.

References

[1] H. Spliethoff, K.R.G. Hein, Effect of co-combustion of biomass on emissions in pulverized fuel furnaces, Fuel Processing Technology, 54 (1998) 189-205.
[2] P. Basu, J. Butler, M.A. Leon, Biomass co-firing options on the emission reduction and electricity generation costs in coal-fired power plants, Renewable Energy, 36 (2011) 282-288.

[3] M. Sami, K. Annamalai, M. Wooldridge, Co-firing of coal and biomass fuel blends, Progress in Energy and Combustion Science, 27 (2001) 171-214.
[4] K. Savolainen, Co-firing of biomass in coal-fired utility boilers, Applied Energy, 74 (2003) 369-381.
[5] A. Demirbas, Combustion characteristics of different biomass fuels, Progress in Energy and Combustion Science, 30 (2004) 219-230.
[6] F. Al-Mansour, J. Zuwala, An evaluation of biomass co-firing in Europe, Biomass and Bioenergy, 34 (2010) 620-629.
[7] A. Malmgren, G. Riley, 5.04 - Biomass Power Generation, in: S. Editor-in-Chief: Ali (Ed.) Comprehensive Renewable Energy, Elsevier, Oxford, 2012, pp. 27-53.
[8] T.F. Wall, R.A. Creelman, R.P. Gupta, S.K. Gupta, C. Coin, A. Lowe, Coal ash fusion temperatures—New characterization techniques, and implications for slagging and fouling, Progress in Energy and Combustion Science, 24 (1998) 345-353.
[9] C. Luan, C. You, D. Zhang, An experimental investigation into the characteristics and deposition mechanism of high-viscosity coal ash, Fuel, 119 (2014) 14-20.
[10] C. Luan, C. You, D. Zhang, Composition and sintering characteristics of ashes from co-firing of coal and biomass in a laboratory-scale drop tube furnace, Energy, 69 (2014) 562-570.
[11] Q.H. Li, Y.G. Zhang, A.H. Meng, L. Li, G.X. Li, Study on ash fusion temperature using original and simulated biomass ashes, Fuel Processing Technology, 107 (2013) 107-112.
[12] S.A. Lolja, H. Haxhi, R. Dhimitri, S. Drushku, A. Malja, Correlation between ash fusion temperatures and chemical composition in Albanian coal ashes, Fuel, 81 (2002) 2257-2261.
[13] B. Liu, Q. He, Z. Jiang, R. Xu, B. Hu, Relationship between coal ash composition and ash fusion temperatures, Fuel, 105 (2013) 293-300.
[14] S.V. Vassilev, D. Baxter, C.G. Vassileva, An overview of the behaviour of biomass during combustion: Part I. Phase-mineral transformations of organic and inorganic matter, Fuel, 112 (2013) 391-449.
[15] R.W. Bryers, Fireside slagging, fouling, and high-temperature corrosion of heat-transfer surface due to impurities in steam-raising fuels, Progress in Energy and Combustion Science, 22 (1996) 29-120.
[16] T.F. Wall, A. Lowe, L.J. Wibberley, I. McC. Stewart, Mineral matter in coal and the thermal performance of large boilers, Progress in Energy and Combustion Science, 5 (1979) 1-29.
[17] F.J. Frandsen, Ash research from Palm Coast, Florida to Banff, Canada: Entry of biomass in modern power boilers, Energy and Fuels, 23 (2009) 3347-3378.
[18] E. Raask, Mineral Impurities in Coal Combustion: Behavior, Problems, and Remedial Measures, Hemisphere Publishing Corporation, 1985.
[19] T.F. Wall, S.P. Bhattacharya, D.K. Zhang, R.P. Gupta, X. He, The properties and thermal effects of ash deposits in coal-fired furnaces, Progress in Energy and Combustion Science, 19 (1993) 487-504.
[20] B.-J. Skrifvars, R. Backman, M. Hupa, 96/05936 Ash chemistry and sintering, Fuel and Energy Abstracts, 37 (1996) 422.
[21] F.E. Huggins, D.A. Kosmack, G.P. Huffman, Correlation between ash-fusion temperatures and ternary equilibrium phase diagrams, Fuel, 60 (1981) 577-584.
[22] E. Jak, Prediction of coal ash fusion temperatures with the F*A*C*T thermodynamic computer package, Fuel, 81 (2002) 1655-1668.
[23] H. Li, N. Yoshihiko, Z. Dong, M. Zhang, Application of the FactSage to Predict the Ash Melting Behavior in Reducing Conditions, Chinese Journal of Chemical Engineering, 14 (2006) 784-789.
[24] K. Akiyama, H. Pak, Y. Takubo, T. Tada, Y. Ueki, R. Yoshiie, I. Naruse, Ash deposition behavior of upgraded brown coal in pulverized coal combustion boiler, Fuel Processing Technology, 92 (2011) 1355-1361.
[25] Z. Yong-chun, Z. Jun-ying, L.I.U. Hong-tao, T. Ji-lin, L.I. Yang, Z. Chu-guang, Thermodynamic equilibrium study of mineral elements evaporation in O2/CO2 recycle combustion, Journal of Fuel Chemistry and Technology, 34 (2006) 641-650.

[26] Y. Zhao, Y. Zhang, S. Bao, T. Chen, J. Han, Calculation of mineral phase and liquid phase formation temperature during roasting of vanadium-bearing stone coal using FactSage software, International Journal of Mineral Processing, 124 (2013) 150-153.
[27] J.C. van Dyk, S. Melzer, A. Sobiecki, Mineral matter transformation during Sasol-Lurgi fixed bed dry bottom gasification – utilization of HT-XRD and FactSage modelling, Minerals Engineering, 19 (2006) 1126-1135.
[28] H.L. Wee, H. Wu, D.-k. Zhang, Heterogeneity of Ash Deposits Formed in a Utility Boiler during PF Combustion†, Energy & Fuels, 21 (2006) 441-450.
[29] CEN/TS 15370-1:2006, Solid biofuels - Method for the determination of ash melting behaviour-Part 1: Characteristic temperatures method in, CEN, 2006.
[30] X.C. Baxter, L.I. Darvell, J.M. Jones, T. Barraclough, N.E. Yates, I. Shield, Study of Miscanthus x giganteus ash composition – Variation with agronomy and assessment method, Fuel, 95 (2012) 50-62.
[31] D. Lindberg, R. Backman, P. Chartrand, M. Hupa, Towards a comprehensive thermodynamic database for ash-forming elements in biomass and waste combustion — Current situation and future developments, Fuel Processing Technology, 105 (2013) 129-141.
[32] C.W. Bale, P. Chartrand, S.A. Degterov, G. Eriksson, K. Hack, R. Ben Mahfoud, J. Melançon, A.D. Pelton, S. Petersen, FactSage thermochemical software and databases, Calphad, 26 (2002) 189-228.
[33] C.W. Bale, E. Bélisle, P. Chartrand, S.A. Decterov, G. Eriksson, K. Hack, I.H. Jung, Y.B. Kang, J. Melançon, A.D. Pelton, C. Robelin, S. Petersen, FactSage thermochemical software and databases — recent developments, Calphad, 33 (2009) 295-311.
[34] J. Barroso, J. Ballester, L.M. Ferrer, S. Jiménez, Study of coal ash deposition in an entrained flow reactor: Influence of coal type, blend composition and operating conditions, Fuel Processing Technology, 87 (2006) 737-752.
[35] D. Vamvuka, D. Zografos, Predicting the behaviour of ash from agricultural wastes during combustion, Fuel, 83 (2004) 2051-2057.
[36] M. Pronobis, Evaluation of the influence of biomass co-combustion on boiler furnace slagging by means of fusibility correlations, Biomass and Bioenergy, 28 (2005) 375-383.
[37] J. Werther, M. Saenger, E.U. Hartge, T. Ogada, Z. Siagi, Combustion of agricultural residues, Progress in Energy and Combustion Science, 26 (2000) 1-27.
[38] L.A. Hansen, F.J. Frandsen, K. Dam-Johansen, S. Henning Sund, Quantification of fusion in ashes from solid fuel combustion, Thermochimica Acta, 326 (1999) 105-117.
[39] S. Arvelakis, P.A. Jensen, K. Dam-Johansen, Simultaneous Thermal Analysis (STA) on Ash from High-Alkali Biomass, Energy & Fuels, 18 (2004) 1066-1076.
[40] S. Du, H. Yang, K. Qian, X. Wang, H. Chen, Fusion and transformation properties of the inorganic components in biomass ash, Fuel, 117, Part B (2014) 1281-1287.
[41] M. Pansu, J. Gautheyrou, Handbook of Soil Analysis: Mineralogical, Organic and Inorganic Methods, Springer London, Limited, 2007.
[42] Q. Zhang, H. Liu, Y. Qian, M. Xu, W. Li, J. Xu, The influence of phosphorus on ash fusion temperature of sludge and coal, Fuel Processing Technology, 110 (2013) 218-226.

Table1. Characteristics of fuels

Description	Wood (Pine)	Peanut shell	Sunflower stalk	Miscanthus husk
Proximate Analysis weight%(dry basis)				
VM	77.95	77.24	77.07	80.16
FC	20.0	19.29	19.98	15.96
Ash	2.05	3.47	2.95	3.88
Elemental Analysis weight%(dry basis)				
C	47.37	45.98	49.10	46.82
H	5.35	5.46	5.60	5.42
N	0.66	2.30	1.65	1.01
O*	44.72	43.06	40.95	43.15
S	[b]	[b]	[b]	[b]

*calculated by difference

[b] below instrument detection limit (<1%)

Table 2. Elemental analysis of ash and calculated indices

% oxide in ash	Wood Pine	Peanut shell	Sunflower stalk	Miscanthus husk
SiO_2	45.229	35.26	3.21	49.55
Al_2O_3	10.60	8.19	0.48	0.45
Fe_2O_3	5.93	3.22	0.84	0.41
K_2O	9.76	30.88	45.10	30.49
CaO	20.04	9.92	27.16	7.95
MgO	4.55	5.12	15.24	2.86
P_2O_5	1.29	4.49	5.30	5.76
SO_3	0.54	0.77	2.43	0.13
Na_2O	1.42	1.32	0.21	2.39
TiO_2	0.64	0.82	0.03	0.01
Indices				
B/A	0.74(H)	1.14(S)	23.75 (S)	0.88(S)
S_R	59 (H)	65 (H)	7 (S)	81 (L)
F_U	8.25(H)	36.7(H)	1076 (S)	29 (H)
AI	0.12(L)	0.57(H)	0.64 (H)	0.65(H)

Table 3. Ash fusion temperatures

Sample	DT(^{0}C)	HT(^{0}C)	FT(^{0}C)
Wood	1095	1210	1235
Peanut shell	1080	1250	1265
Sunflower husk	1225	1515	1560
Miscanthus	835	1020	1040

Table 4. Minimum endotherm temperatures from DTA curves

Ash Sample	Minimum Endotherm Temperature (^{0}C)
Wood(Pine)	980
Peanut shell	1060
Sunflower Husk	940
Miscanthus	750

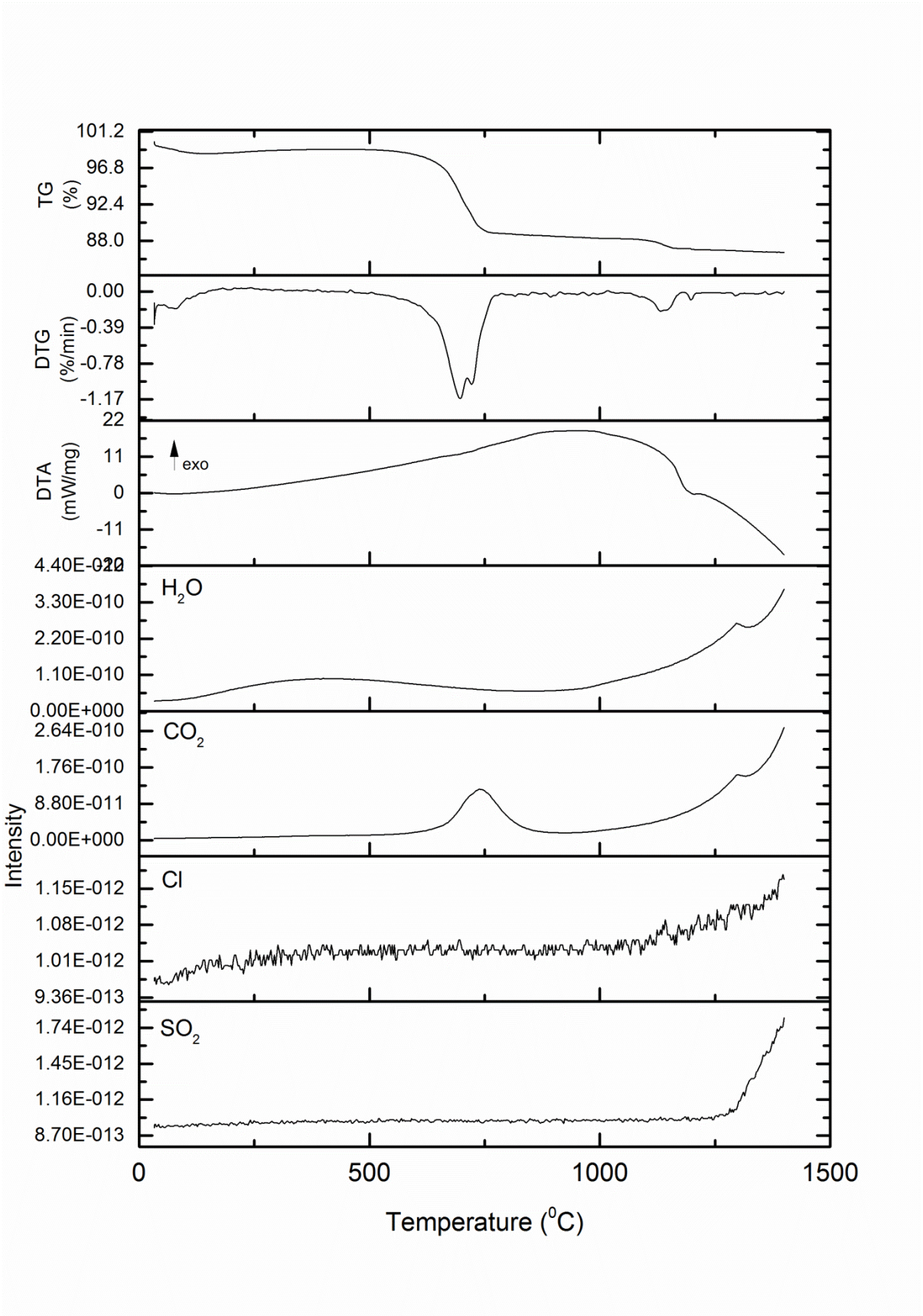

Figure 1. STA-MS curves for wood ash.

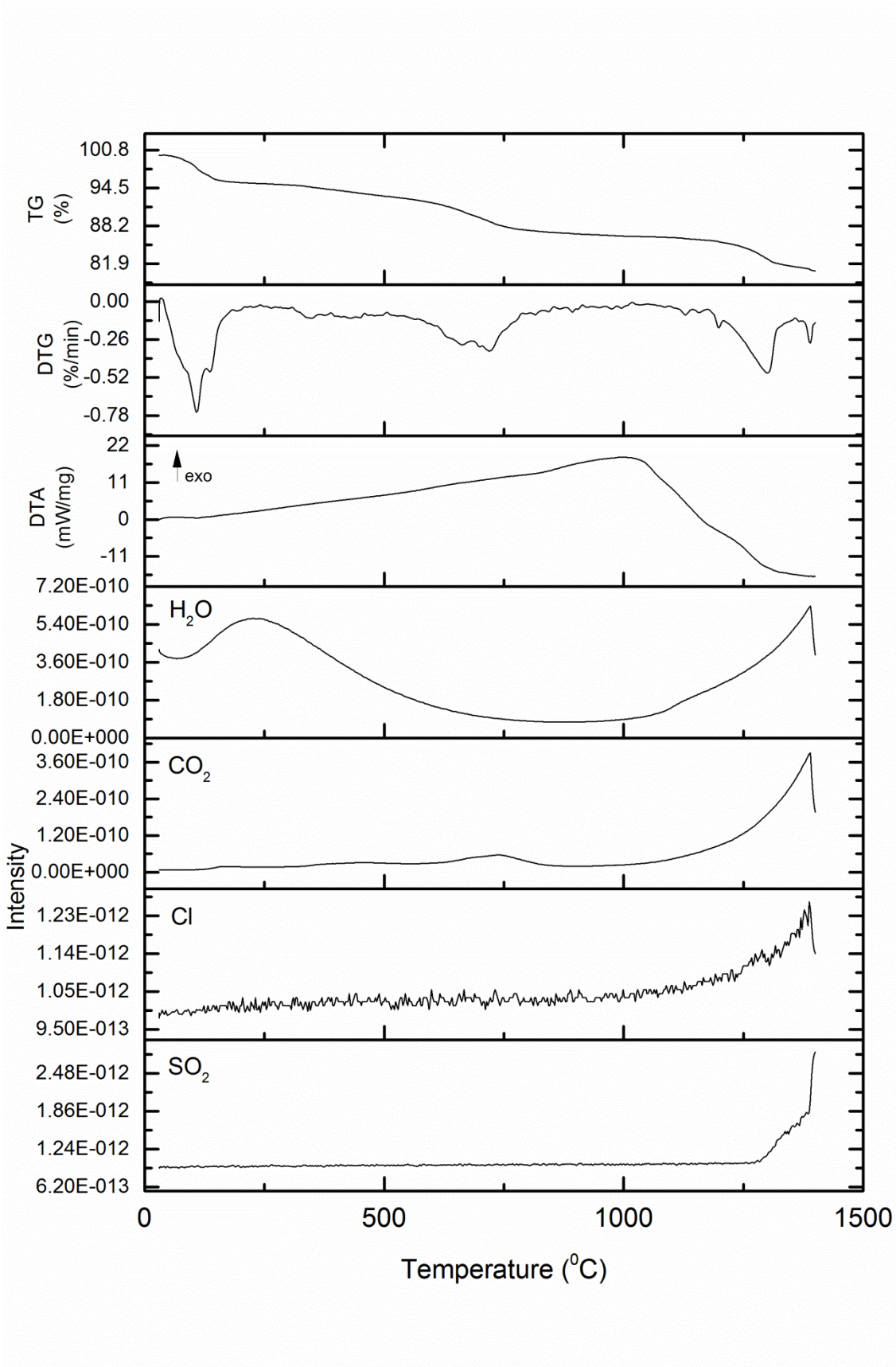

Figure 2. STA-MS curves for peanut ash.

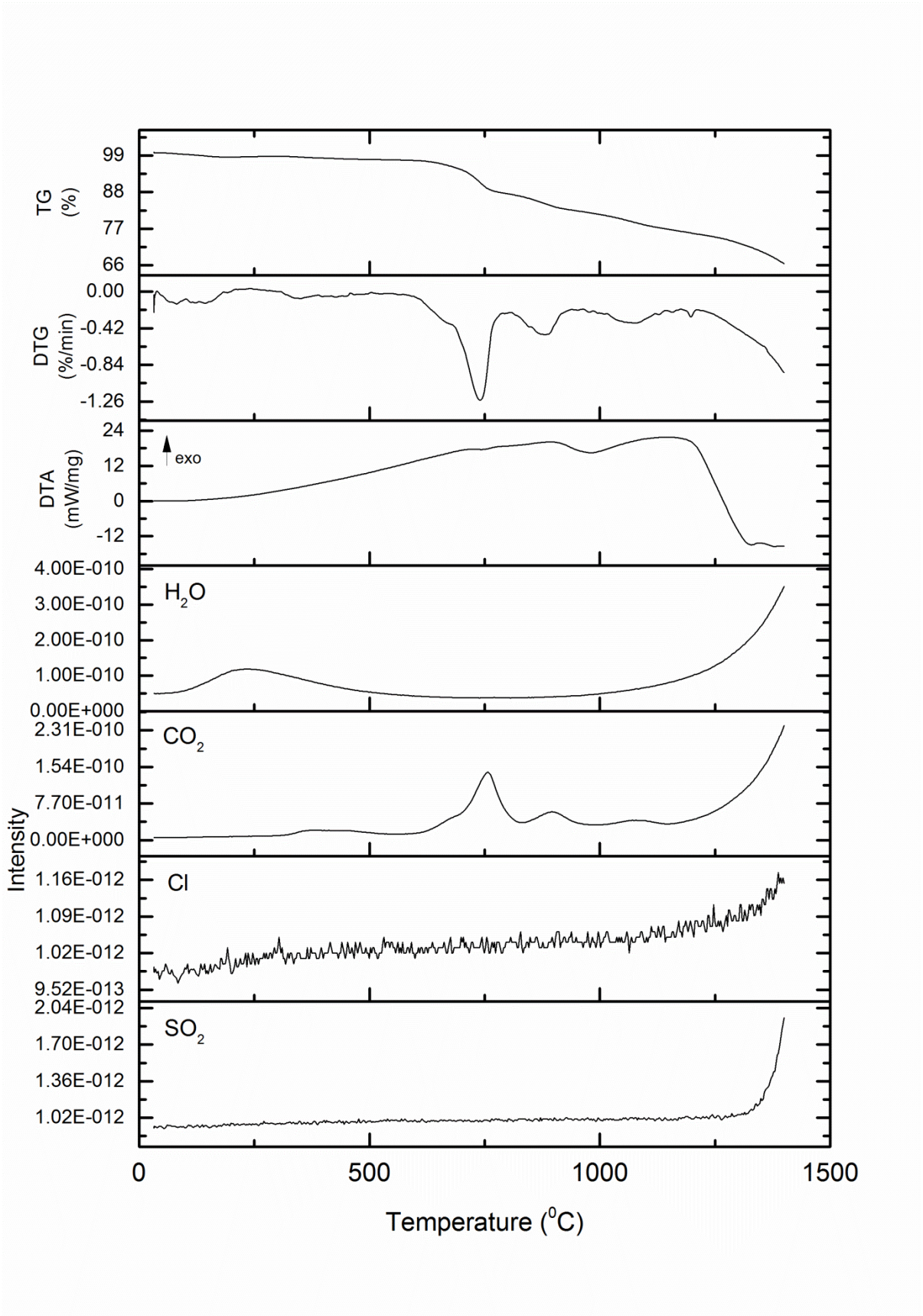

Figure 3. STA-MS curves for sunflower ash.

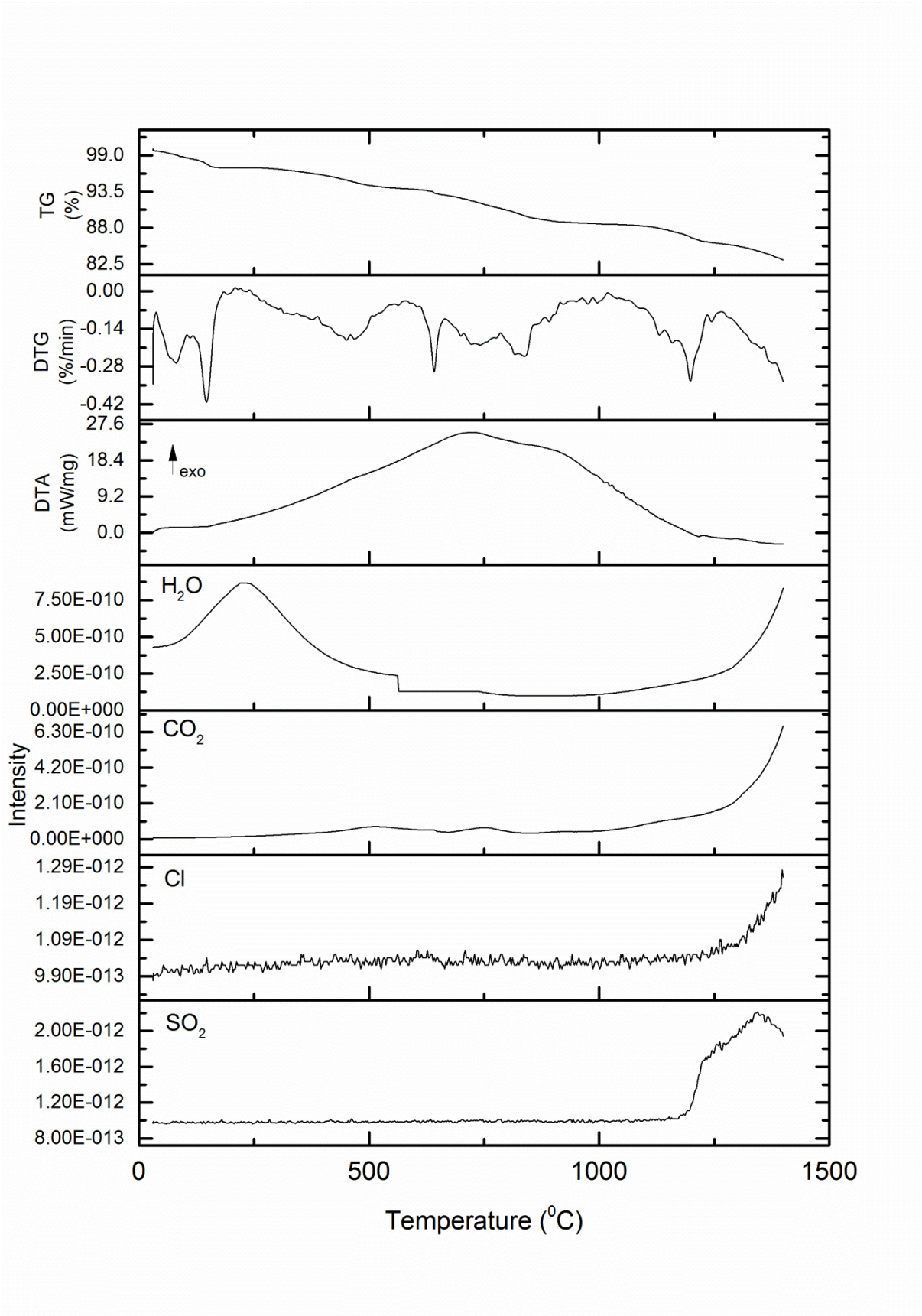

Figure 4. STA-MS curves for miscanthus ash.

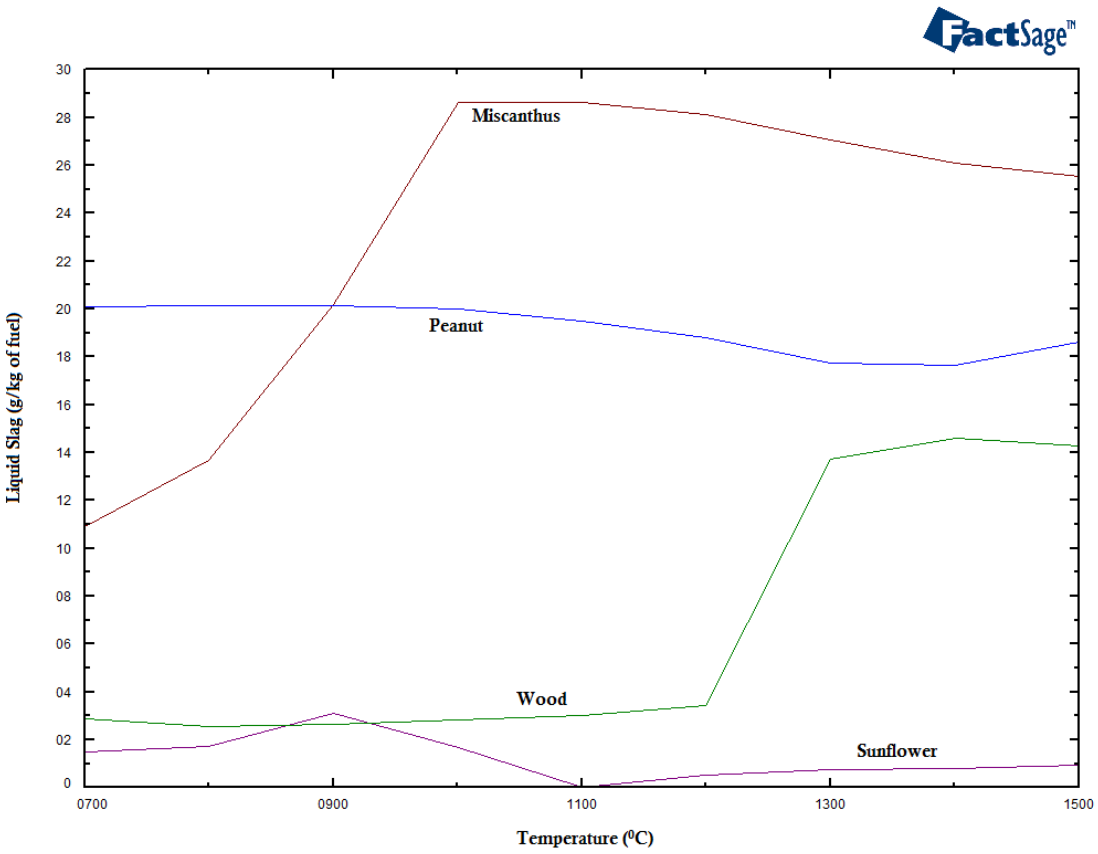

Figure 5. Liquid slag formation at different temperatures calculated using Factsage 6.3.

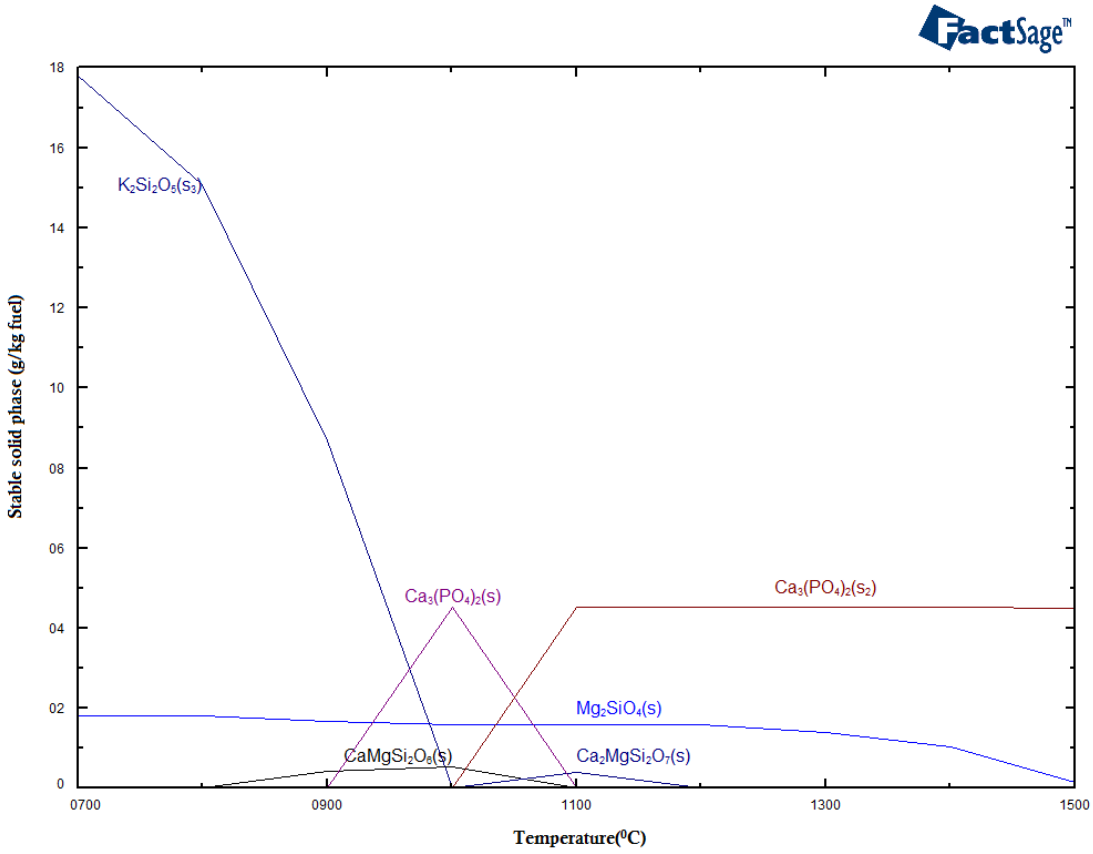

Figure 6(a). Stable solid phases in equilibrium with the slag phase for Miscanthus ash.

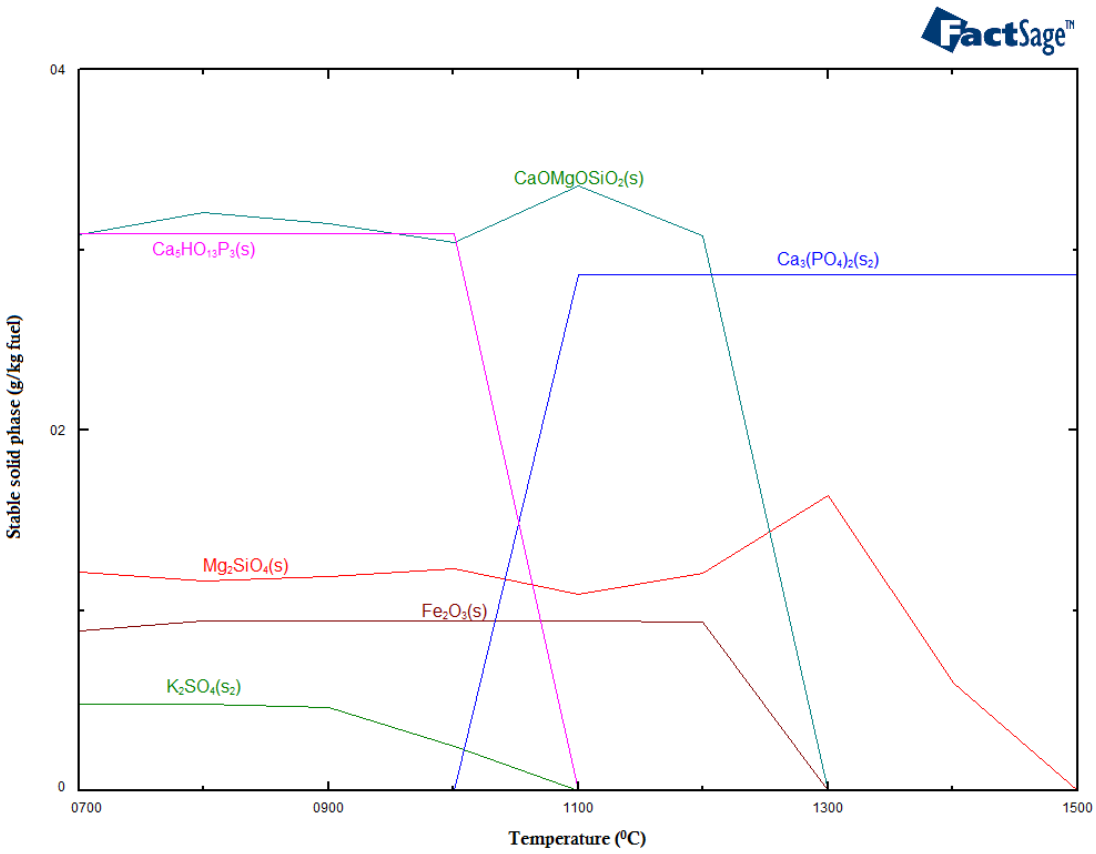

Figure 6(b). Stable solid phases in equilibrium with the slag phase for Peanut ash.

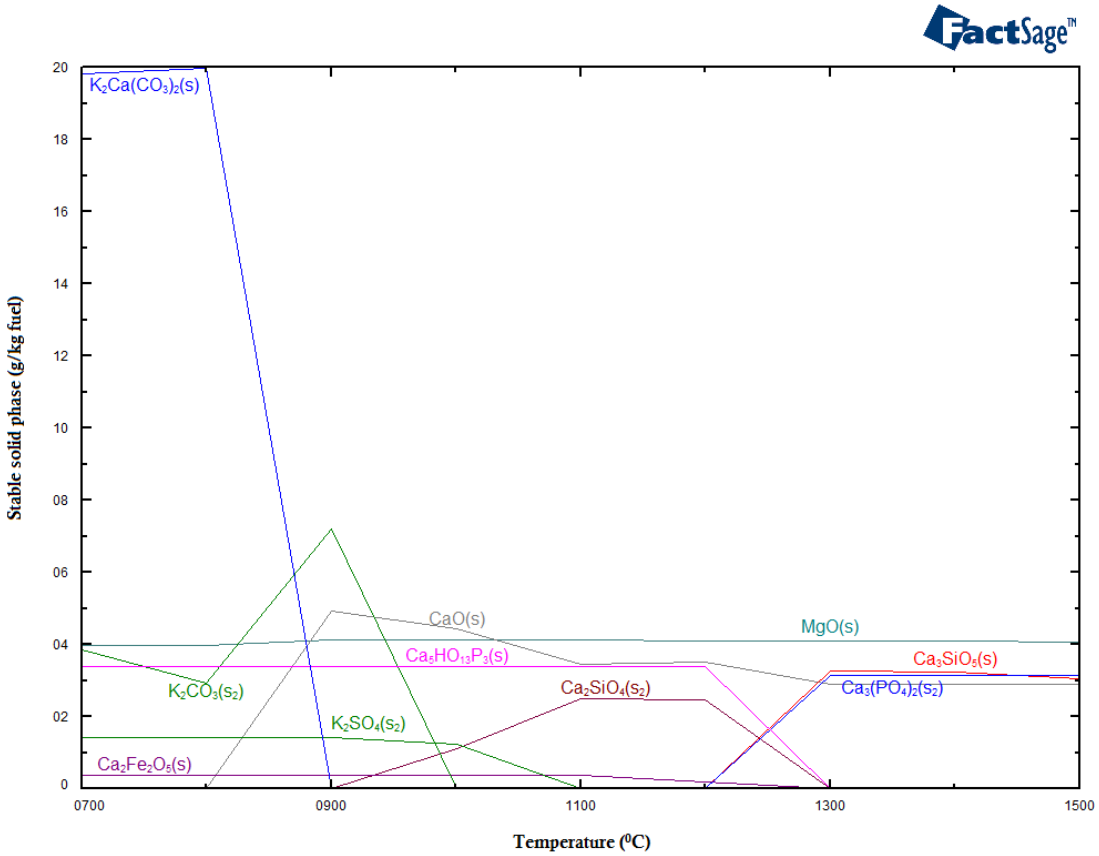

Figure 6(c). Stable solid phases in equilibrium with the slag phase for Sunflower ash.

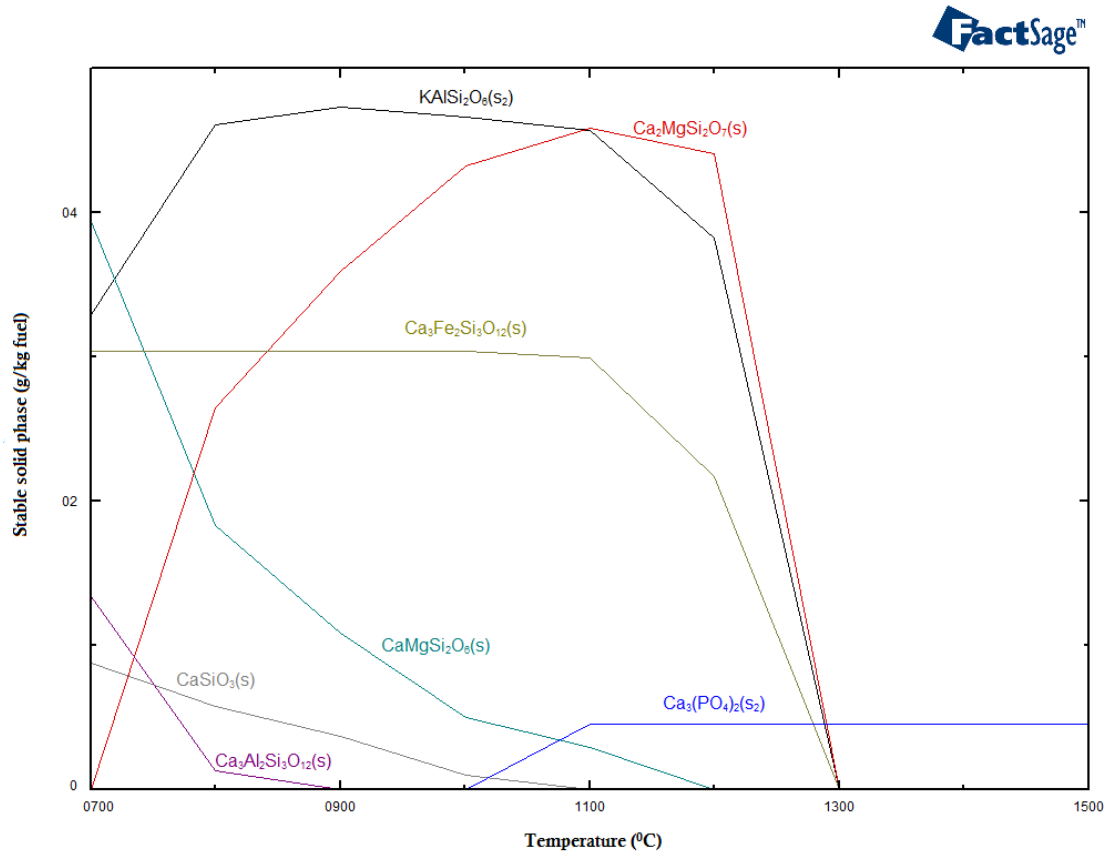

Figure 6(d). Stable solid phases in equilibrium with the slag phase for Wood ash.

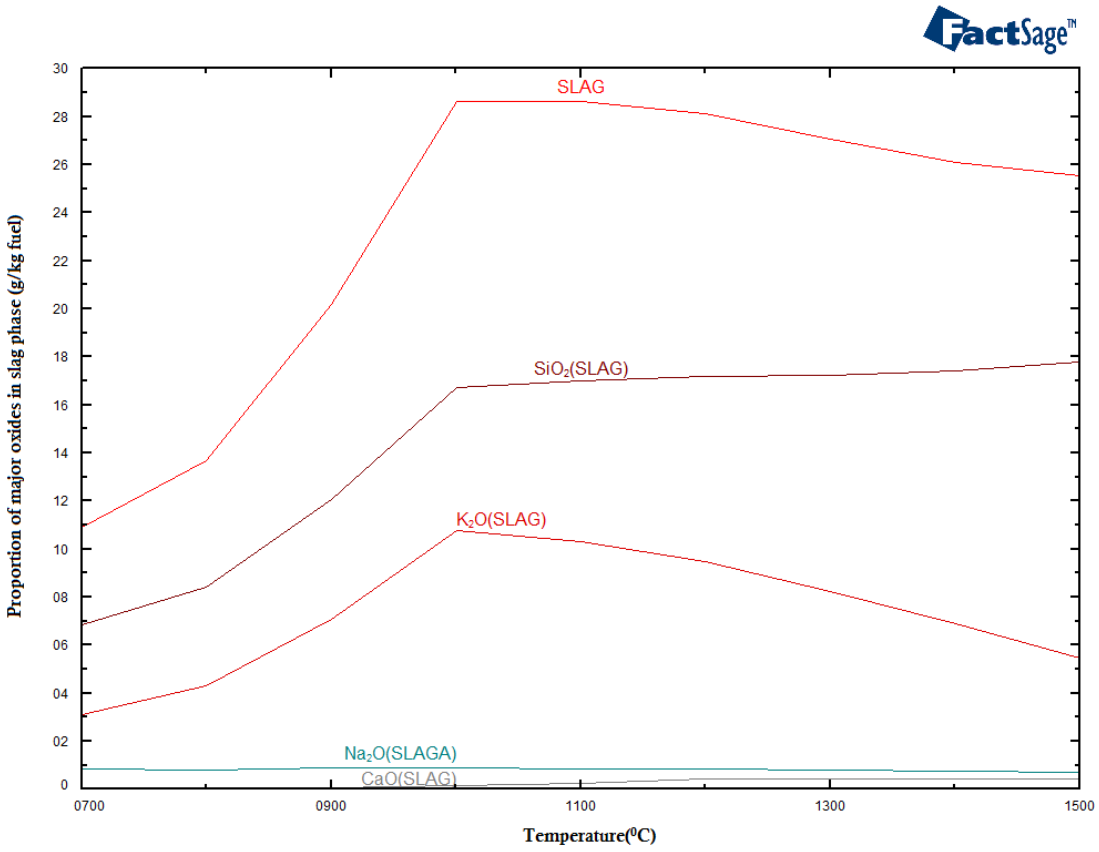

Figure 7(a). Proportion of major oxides in the slag phase for Miscanthus ash.

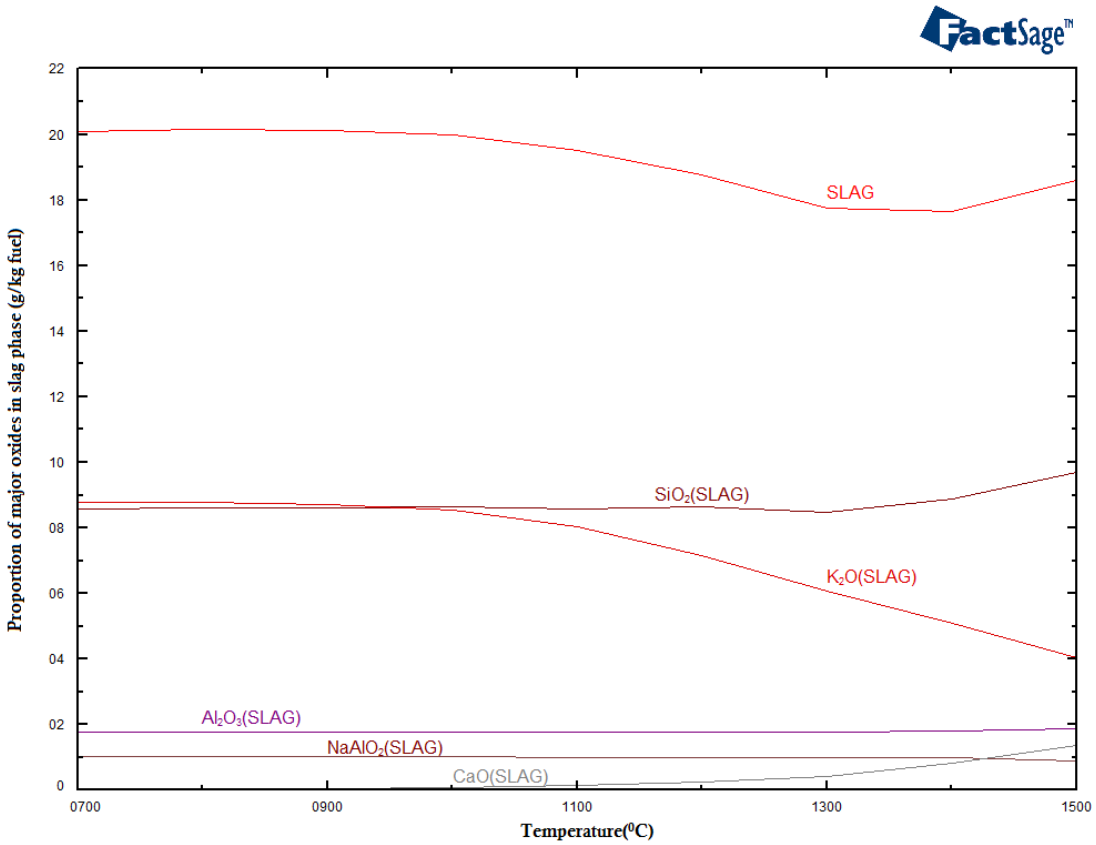

Figure 7(b). Proportion of major oxides in the slag phase for Peanut ash.

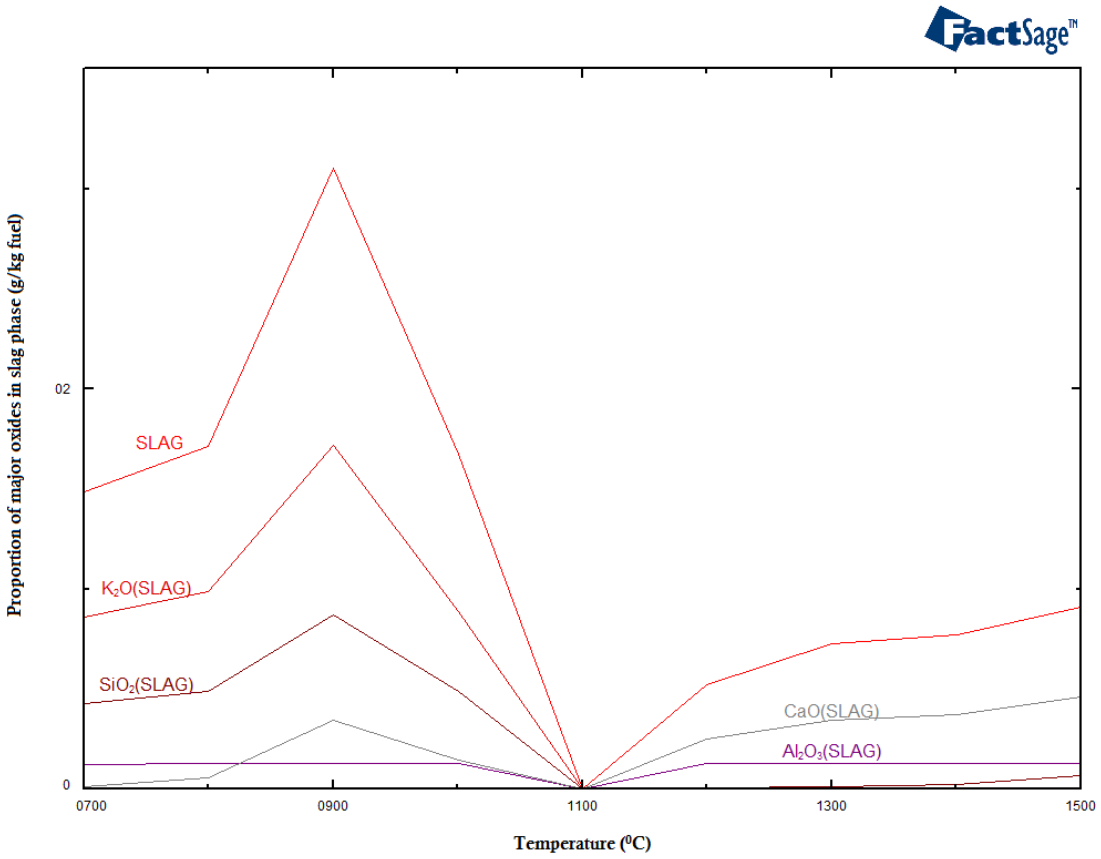

Figure 7(c). Proportion of major oxides in the slag phase for Sunflower ash.

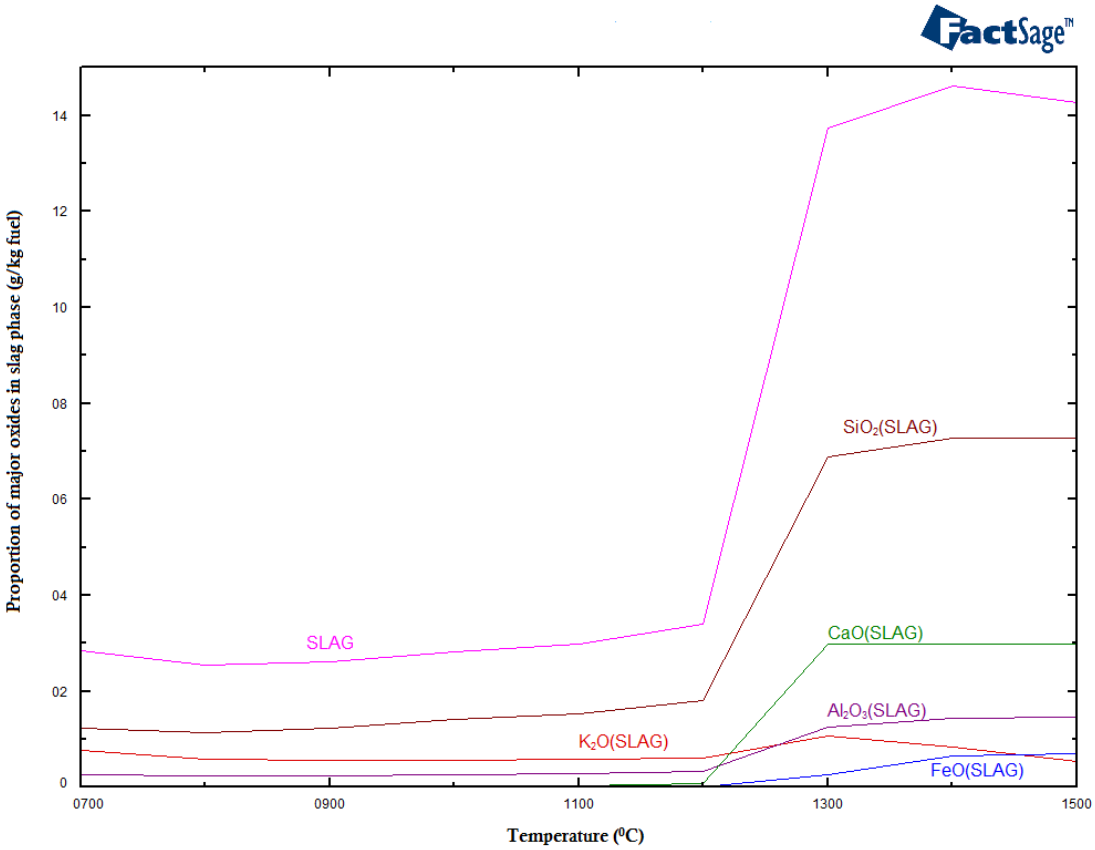

Figure 7(d). Proportion of major oxides in the slag phase for Wood ash.